The hemopexin domain of MMP-9 inhibits angiogenesis and retards growth of intracranial glioblastoma xenografts in nude mice. Int J Cancer

ARTICLE *in* INTERNATIONAL JOURNAL OF CANCER · JANUARY 2009

Impact Factor: 5.09 · DOI: 10.1002/ijc.23951 · Source: PubMed

Published in final edited form as:
Int J Cancer. 2009 January 15; 124(2): 306–315. doi:10.1002/ijc.23951.

The hemopexin domain of MMP-9 inhibits angiogenesis and retards the growth of intracranial glioblastoma xenograft in nude mice

Ravesanker Ezhilarasan[1], **Unmesh Jadhav**[1], **Indra Mohanam**[1], **Jasti S. Rao**[1,2], **Meena Gujrati**[3], and **Sanjeeva Mohanam**[1]

[1]Department of Cancer Biology and Pharmacology, University of Illinois College of Medicine, Peoria IL 61605 USA

[2]Department of Neurosurgery University of Illinois College of Medicine, Peoria IL 61605 USA

[3]Department of Pathology University of Illinois College of Medicine, Peoria IL 61605 USA

Abstract

Matrix Metalloproteinase-9 (MMP-9) consists of a prodomain, catalytic domain with three fibronectin-like type II modules and C-terminal hemopexin-like (PEX) domain. These domains play distinct roles in terms of proteolytic activity, substrate binding and interaction with inhibitors and receptors. In order to assess the potential of the MMP-9-PEX domain to interfere with tumor progression, we stably transfected human glioblastoma cells with an expression vector containing a cDNA sequence of the MMP-9-PEX. The selected clones exhibited decreased MMP-9 activity and reduced invasive capacity. We assessed how secretion of MMP-9-PEX by glioblastoma cells affects angiogenic capabilities of human microvascular endothelial cells (HMECs) *in vitro*. MMP-9-PEX conditioned medium treatment caused a reduction in migration of human microvascular endothelial cells (HMECs) and inhibited capillary-like structure formation in association with suppression of vascular endothelial growth factor (VEGF) secretion and VEGF receptor-2 protein level. The suppression of HMECs survival by conditioned medium from MMP-9-PEX stable transfectants was associated with apoptosis induction characterized by an increase in cells with a sub-G_0/G_1 content, fragmentation of DNA, caspase-3, -8 and -9 activation and poly (ADP-ribose) polymerase (PARP) cleavage. A significant tumor growth inhibition was observed in intracranial implants of MMP-9-PEX stable transfectants in nude mice with attenuation of CD31 and MMP-9 protein expression. These results demonstrate that MMP-9-PEX inhibits angiogenic features of endothelial cells and retards intracranial glioblastoma growth.

Keywords

MMP-9; glioblastoma; angiogenesis; tumor growth inhibition

Introduction

Glioblastomas are the most common and malignant central nervous system tumors.1 Current therapeutic modalities include combinations of surgery, radiotherapy, and chemotherapy; however these therapies remain ineffective and patients with glioblastoma multiforme have a median survival time of less than one year.2–4 Glioblastomas are very aggressive,

Corresponding to: Sanjeeva Mohanam Ph.D. Department of Cancer Biology and Pharmacology, University of Illinois College of Medicine, Peoria IL 61656, USA. Fax: 309-671-3442; smohanam@uic.edu.

characterized by a high proliferation rate, extensive angiogenesis, and marked tumor cell invasion into normal brain parenchyma.[4, 5] The process of neovascularization involves a complex series of sequential events targeted in the activation of matrix degrading enzymes and motility.[6,7] MMP-2 and MMP-9 play an important role in degradation of extracellular matrix components and are involved in a multitude of physiological and pathological processes.[8–10] MMP-2 and MMP-9 are the two most abundant MMPs found in gliomas.[11–13] Like most MMPs, MMP-2 and MMP-9 contain an N-terminal pro-domain, catalytic zinc-binding domain and the C-terminal PEX domain [9,14] but differ from other MMPs by containing three- fibronectin type II repeats within the catalytic domain.[15]

The PEX domain of various MMPs has been reported to have biological activities independent of the full-length enzyme.[16–18]. MMP-2-PEX has a role in binding substrates, inhibitors and receptors.[19–23]. MMP-2-PEX acts as an inhibitor of glioma angiogenesis, cell proliferation, and migration.[24, 25]. MMP-9-PEX contains the binding site for tissue inhibitor of MMP-1 (TIMP-1), low density lipoprotein receptor-related protein 1 (LRP-1) and megalin/LRP-2 and mediates the dimerization of MMP-9.[26–28] MMP-9-PEX reduces MMP-9 activity *in vitro* and inhibits invasion of predominantly MMP-9 expressing malignant human melanoma cells but not of rat mesangial cells expressing MMP-2 exclusively.[18] However the effects of MMP-9-PEX *in vivo* have not yet been studied. In this study, we report evidence that the enforced secretion of MMP-9-PEX in human glioblastoma cells suppresses angiogenic features of endothelial cells and inhibits intracranial tumor growth providing a novel therapeutic approach for glioblastoma.

Materials and methods

Cell culture

The human glioblastoma SNB19 cells were cultured in DMEM supplemented with 10% FBS, penicillin (100 units/ml), and streptomycin (100 μg/ml). Human microvascular endothelial cells (HMECs) were maintained as described earlier.[29] Tumor cell conditioned medium was prepared from the SNB19 cell culture grown to near confluency. After being washed twice with serum free medium, SNB19 cells were incubated in serum free MCDB medium for 24-h. The conditioned medium was harvested, centrifuged at 2000 × g at 4°C for 10 min and supplemented with EGF and hydrocortisone prior to use in HMECs.

Vector construction and transfection

The MMP-9-PEX expression construct, the signal sequence (N-terminal Met_1–Ala_{20}) fused with the hemopexin domain (Thr_{506}–Asp_{707}) was generated using overlap extension PCR. In the first step, the signal sequence was amplified using the primer pair A/B (primer A, 5'-CTGAATTCACCATGAGCCTCTGGC-3'; primer B, 5'-ACTCAAA GGCACAGTGGCAGCAAAGCAGCAG-3') and the hemopexin domain sequence was amplified using the primer pair C/D (primer C, 5'-CTGCTGCTTTGCTGCCACTGTG CCTTTGAGTCC-3'; primer D, 5'-AGCTCG AGTCCTCAGGGCACTG-3') separately. In second step, Primer pair A/D was then used to link the two PCR products for each construct by the overlap extension techniques. The resulting MMP-9 PEX was then cloned into the pcDNA3.1/V5-His-TOPO vector, which contains the C-terminal hexahistidine tag. Stable clones of SNB19 cells expressing MMP-9-PEX were then established as described elsewhere.[30] The secretion of MMP-9 PEX was tested by western blot analysis with an antibody derived against the MMP-9 (sc-21733; Santa Cruz Biotechnology, Santa Cruz, CA) or hexahistidine tag (Cell Signaling, Beverly, MA). Further, MMP-9-PEX was purified from serum-free medium collected from stable transfectant (PX-1) using HisPur Cobalt Resin (Thermo Scientific, Lafayette, CO) according to manufacturer's instructions and the homogeneity was confirmed by western blotting analysis. Parental cells, vector alone and

MMP-9 PEX transfectants were further transfected by standard protocols with Fugene 6 (GE Healthcare Life Sciences, Arlington Heights, IL) using a phCMV-Luc (Genlantis, San Diego, CA) expression vector. After expansion, clones were tested for luciferase expression and one clone of parental cells (PLuc) vector alone (VC-Luc) and MMP-9-PEX transfectants (PX1-Luc, PX2-Luc) showing the highest luminescence activity was then selected and plated out at limiting dilution. A single clone was isolated again and verified for luciferase activity to ensure a true clonal population and tested *in vivo* for intracranial growth behavior.

SDS-PAGE and western blot analysis

Cells were lysed in ice-cold lysis buffer solution containing protease inhibitors and total proteins were extracted as described previously.31 Samples were subjected to SDS-PAGE and separated proteins were transferred onto membrane followed by blocking of membrane with 5% Non-fat milk powder (w/v) in tris- buffered saline (10 mM Tris, 100 mM NaCl, 0.1% Tween 20) for 1-h at room temperature or overnight at 4°C. Membranes were probed using specific primary antibodies followed by appropriate secondary antibody and enhanced chemiluminescence visualization. Membranes were stripped and reprobed with GAPDH antibody (Novus Biologicals, Littleton, CO) as a protein loading control.

Gelatin zymography

To measure the activity of MMPs, the conditioned medium was incubated with non-reducing buffer before electrophoresis on a 10% SDS-polyacrylamide gel containing 0.1% gelatin. Following electrophoresis, the gel was washed twice in 2.5% Triton X-100 to remove the SDS followed by incubation overnight at 37°C in 50 mM Tris-HCl, 10 mM $CaCl_2$, buffer (pH 7.6) that allows both pro-gelatinase and active gelatinase to digest the gelatin. The gel was then stained with amido black to visualize gelatinolytic activity.

In vitro invasion Assay

Cells were seeded onto the Transwell membranes (6.5 mm in diameter and 8-μm pores) coated with Matrigel.30 After a 24-h incubation period, cells remaining on the upper face of the membranes were removed with a cotton swab and those on the lower face were fixed with methanol, stained with crystal violet for 15 min, counted using an inverted microscope and the percentage of cells that had migrated through the Matrigel was determined.

In vitro angiogenesis assay

Matrigel basement membrane matrix (Becton Dickinson) was plated into flat-bottomed 96-well tissue culture plates and then incubated at 37°C for 20 min to allow the Matrigel to polymerize before HMECs were added with conditioned medium from SNB19 stable transfectants. This assay was also performed using purified MMP-9-PEX (PX1) protein with and without active recombinant MMP-9 (Calbiochem, San Diego, CA). After 24-h incubation period at 37°C in a humidified 5% CO_2 atmosphere, capillary tube formation was observed, images were taken with a phase contrast microscope and quantitative evaluation of the capillary tubes was done by computer-assisted image analysis with the Image-Pro Discovery program.

RNA Extraction and Quantification by Real-time PCR

Total RNA was extracted from cultured cells using TRIzol reagent (Invitrogen, Carlsbad, CA) and reverse-transcribed using the cDNA cycle kit (Invitrogen Carlsbad, CA) with random primers following the instructions of the manufacturer. The cDNA was subjected to PCR amplification using IQ SYBR green Supermix (Bio-Rad, Hercules, CA) and real-time

detection on iCycler (Bio-Rad) PCR machine. The forward (F) and reverse (R) primers used were: 5'-GCAGTGCAATACCTGAACACCTTC-3' (F)

5'-CCATACTTCACACGGACCACTTG-3' (R) for MMP-2

5'-TGGACGATGCCTGCAACGTG-3' (F)

5'-GTCGTGCGTGTCCAAAGGCA-3' (R) for MMP-9

5′-AGCCTTGCCTTGCTGCTCTA-3′ (F) and

5′-GTGCTGGCCTTGGTGAGG -3′ (R) for $VEGF^{165}$,

5′-CTGGCATGGTCTTCTGTGAAGCA-3′ (F) and

5′-AATACCAGTGGATGTGATGCGG-3′ (R) for VEGFR-2

5'-TCTACAATGAGCTGCGTGTGGCTCC-3' (F)

5'-AGGAAGGAAGGCTGGAAGAGTGCCTC-3' (R) for β-actin. All samples were run in triplicate for each gene assayed. The steady-state concentration of mRNA for MMP-2, MMP-9, VEGF and VEGFR2 in endothelial cells was quantitated using the comparative C_T method and normalized to the amount of β-actin mRNA.

ELISA

Commercial ELISA kits were used and assays were done according to the manufacturer's instructions to measure concentrations of VEGF (R&D Systems, Minneapolis, MN) in conditioned media of the 24-h and 48-h endothelial cell cultures after normalization for total protein. Cell lysates were used to determine VEGFR2 levels by ELISA (R&D Systems). Three ELISA experiments were conducted, with each sample done in duplicate.

Wound-Induced migration Assay

Cells were grown to confluency and a scratch was made through the cell monolayer using a pipette tip. After washing with PBS, fresh culture medium was added. Photographs of the wounded area were taken after 24-h by staining with crystal violet to monitor the invasion of cells into the wounded area and the distance that the advancing cells had moved into the cell-free (wounded) area was measured.

Cell migration from spheroids

Migration from spheroids was assayed as described previously.31 Single multicellular spheroids of HMECs were placed in the center of each well of a 96-well microplate and were cultured for 24-h, after which the spheroids were fixed and stained with crystal violet and cellular migration from the spheroids was assessed under light microscopy.

DNA Cell Cycle Analysis

Cells were harvested, washed once with PBS, and fixed in 3.7% paraformaldehyde in PBS for 10 min at room temperature. Cells were pelleted, washed once with PBS, and resuspended in a PI solution (50 μ g/ml PI, Sigma; 0.1 mg/ml RNase A in PBS, pH 7.4) for 30 min in the dark. Flow cytometry analysis was performed using FASCalibur flow cytometry system (BD Biosciences San Jose, CA) as described previously.31 The percentages of cells within the G_1, S, and G_2/M phases of the cell cycle were determined by analysis with the program CellQuest.

Hoechst 33258 staining

Endothelial cells were cultured in the presence of SNB19 conditioned medium for 24-h. Then, cells were washed with PBS and fixed with formalin in PBS. After fixation, cells were stained with Hoechst 33258 (1 μg/ml, Molecular Probes, Eugene, OR) for 10 min at 37 °C in the dark. Cells were washed twice with PBS and were analyzed under a fluorescent microscope (Olympus IX 70). Apoptotic cells were identified by nuclear condensation, formation of membrane blebs and apoptotic bodies.

Intracranial implantation of tumor cells

Nude mice at four to six weeks of age were anaesthetized, placed in a stereotactic frame (David Kopf Instruments, Tujunga, CA) and injected with 1×10^6 tumor cells in 10 μl of PBS through a 27-gauge needle at 2 mm lateral and posterior to the bregma and 3 mm below the dura. Tumor cells were allowed to engraft and in vivo bioluminescence imaging was performed to assess tumor growth. After 28 days, mice were sacrificed and their brains were harvested, embedded in OCT, and stored at −70°C. Sections (10 μm) were stained with H&E using standard protocols.

Bioluminescence imaging

Intracranial tumor growth using bioluminescence was assed via Xenogen IVIS 200 small-animal imaging system (Xenogen, Alameda, CA). Tumor bearing animals were injected i.p. with 50 mg/kg luciferin (Gold Biotechnology, St Louis, MO) in PBS. During image recording, mice inhaled isofluorane delivered via a nose cone and their body temperature was maintained at 37 °C in the dark box of the camera system. Bioluminescence images were recorded between 10 and 20-min post luciferin administration. The bioluminescence intensity was quantified with the LivingImage software (Xenogen) as an overlay on IGOR (Wavemetrics, Seattle, WA, USA). Signal intensity was quantified as the sum of detected photons per second within the region of interest using the LivingImage software package.

Immunohistochemistry

Tumors derived from control and PEX transfectants implanted mice were dissected, embedded in OTC, snap-frozen and 5–6μm sections were cut with a cryostat. Sections were treated for 10 min with 3% H_2O_2 in phosphate-buffered saline to block endogenous peroxidases. They were incubated with 2.5% BSA in PBS to block any nonspecific binding. For anti-CD31 (sc-8306; Santa Cruz Biotechnology, Santa Cruz, CA), and anti-MMP-9 (Biomeda, Foster City, CA) immunohistochemistry, sections were incubated with primary antibodies for 1 hour (rabbit polyclonal antibodies). Then, immunoreactive complexes were detected using the corresponding secondary biotin-conjugated antibodies augmented by streptavidin/horseradish peroxide and visualized by 3-amino-9-ethyl-carbazole (Biomeda, Foster City, CA), which gives a red brown reaction product. The tumor sections were counterstained with hematoxylin. Controls included omission of the primary antibody and incubation with normal rabbit immunoglobulin or normal rabbit serum before staining.

Statistical analysis

Statistical significance of the experimental results was determined by the Student's t-test. For all analyses $p < 0.05$ was accepted as a significant probability level.

Results

Generation of MMP-9-PEX Expressing SNB19 Cell Lines

After transfecting SNB19 cells with pcDNA3.1/V5-His vector containing MMP-9-PEX construct using Fugene 6 and their selection with G418, cell lines stably expressing MMP-9-

PEX were established. Western blot analysis was performed on conditioned media collected from SNB19 and G418 resistant clones as well as HisPur cobalt resin-purified MMP-9-PEX protein using antibodies against MMP-9 C-terminal domain and His protein to determine whether MMP-9-PEX cDNA transfection results in protein expression in stable transfectants (Fig1a, 2c). Cell lines transfected with MMP-9-PEX expression vector showed MMP-9-PEX protein secretion whereas parental and vector-alone transfectants did not reveal any band corresponding to MMP-9-PEX as expected. These results clearly show that MMP-9-PEX protein secretion was due to MMP-9-PEX cDNA expression. No impaired growth or increased apoptosis was found in MMP-9 stable transfectants compared with controls (data not shown).

Endogenous MMP-9-PEX secretion reduces MMP-9 activity and in vitro invasion

It is intriguing to know whether endogenously expressed MMP-9-PEX interferes with MMP-9 activity. To clarify this, conditioned media collected from phorbol myristate acetate (PMA)-treated parental and stable transfectants were analyzed for MMP-9 activity using gelatin zymography. Fig1b demonstrates that MMP-9 activity was decreased significantly in stable MMP-9-PEX transfectants compared to parental and vector controls. Since MMP-9-PEX inhibits MMP-9 activity, we assessed its ability to inhibit cell invasion *in vitro*. The effect of endogenous MMP-9-PEX expression on the invasiveness of SNB19 cells was studied using *in vitro* Matrigel invasion assay. We found no marked difference in invasion between parental and vector transfectants; however a significant inhibition in invasive potential was noted in MMP-9-PEX transfected clones (Fig1c). Quantitative analysis of cells invaded through the Matrigel showed a significant reduction in MMP-9-PEX stable transfectants compared to the vector-alone transfected control (Fig1d).

MMP-9-PEX on inhibition of in vitro angiogenesis

The effect of MMP-9-PEX on angiogenesis was determined via *in vitro* angiogenesis assays. HMECs develop capillary-like structures when plated onto Matrigel and maintained. We checked whether capillary formation is modulated by MMP-9-PEX. While parental and vector-alone conditioned medium treated HMECs formed capillary-like network structures on Matrigel surfaces, this network-forming ability was lost in HMECs cultured in presence of MMP-9-PEX conditioned medium (Fig 2a,b). Similar results were obtained in studies performed using purified MMP-9-PEX protein (Fig 2d,e). Further, addition of exogenous recombinant MMP-9 partially reversed the inhibition caused by MMP-9-PEX protein (Fig 2d, e). In order to see if the above-mentioned decrease in capillary-like network formation correlates with changes in the expression of proangiogenic genes, we studied the gene expression of MMP-2, MMP-9, VEGF and VEGFR2 in HMECs treated with vector alone conditioned medium or MMP-9-PEX conditioned medium using real-time RT-PCR. Decreased expression of MMP-9, VEGF and VEGFR2 transcripts was detected in HMECs treated with MMP-9-PEX conditioned medium as compared to vector-control medium treated cells (Fig 3b–d). MMP-9-PEX has no marked effect on the expression of MMP-2 mRNA transcript. Additionally, we performed ELISA to measure the levels of VEGF and VEGFR2 protein. MMP-9-PEX conditioned medium treatment significantly reduced the VEGF and VEGFR2 protein levels in HMECs (Figure 3e, f).

MMP-9-PEX decreases migration of HMECs

We investigated the effects of MMP-9-PEX on angiogenesis-related properties of HMECs. We used tumor-conditioned medium collected from MMP-9-PEX stable transfectants to evaluate the migration of HMECs in three-dimensional spheroid migration and scrape-wound migration assays. Single multicellular spheroids of HMECs were cultured for 24-h in the presence of EC medium or conditioned medium collected from transfected SNB19 cells and cellular migration from the spheroids was assessed under light microscopy. Spheroids of

endothelial cells cultured in the presence of MMP-9-PEX conditioned medium had a significantly smaller area of migrating cells compared with spheroids of vector-alone conditioned medium treated endothelial cells (Fig 4a,b). In a wound-induced migration assay, the subconfluent cell monolayer was disrupted and cells were allowed to migrate into the cell-free area. The mobility of HMECs treated with MMP-9-PEX conditioned medium was decreased in the wound-induced migration assay as compared with vector-alone conditioned medium treated cells (Fig 4c, d).

MMP-9-PEX induces apoptosis of endothelial cells

To assess whether MMP-9-PEX might be involved in induction of apoptosis, cell cycle and apoptosis analysis were performed in HMECs grown in conditioned medium collected from SNB19 stable transfectants. Presented in Fig 5a are representative DNA histograms obtained by flow cytometry that describe the cell cycle distributions of HMECs exposed to tumor cell conditioned medium for 24-h. As shown in figure 5a, exposure of HMECs with MMP-9-PEX conditioned medium resulted in a significantly higher number of cells in the sub G_0-G_1 phase compared with vector-alone conditioned medium treated control. To further analyze the growth inhibitory effect of MMP-9-PEX, we exposed HMECs to tumor cell conditioned medium for 24-h and then analyzed the cells by fluorescence microscopy following Hoechst 33258 staining. In HMECs grown in vector-alone conditioned medium, few apoptotic cells were observed. In contrast, in HMECs grown in the presence of MMP-9-PEX conditioned medium, significant morphological changes and chromosomal condensation occurred, which is indicative of apoptotic cell death (Fig 5b, c). Exposure of HMECs to MMP-9-PEX conditioned medium significantly induced apoptosis in both apoptosis detection methods used.

Role of PEX on caspase activation in HMECs

The expression of proteins related to apoptosis was studied to confirm apoptotic events induced by the MMP-9-PEX in HMECs. Caspase activation is central in apoptosis induction. Caspase-3 is a critical downstream protease in the apoptotic cascade, 32, 33 which is involved in cell death in response to numerous apoptotic stimuli. Therefore, we investigated whether MMP-9-PEX treatment caused its activation. Cleavage of caspases is directly related to their activation status. As shown in Fig 6a, MMP-9-PEX caused an increase of caspase-3 activation. Since caspase-3 activity is increased in both the mitochondrial-mediated and independent apoptotic pathways, we next tested whether MMP-9-PEX would activate either of these pathways. Similarly to that observed with caspase-3 activation, western blot analysis demonstrated cleavage of both procaspase-8 and procaspase-9 to their respective active subunits in HMECs incubated in conditioned medium from MMP-9-PEX stable transfectants (Fig 6b, c). PARP, a downstream target of caspase-3, was also cleaved in cell lines treated with MMP-9-PEX conditioned medium, a hallmark of cells undergoing apoptosis (Fig 6d). Equal protein loading was confirmed by probing the same membrane with GAPDH antibody. Taken together, these results clearly indicate that activation of caspases play a critical role in MMP-9-PEX induced apoptosis in HMECs.

Expression of MMP-9-PEX reduces tumor growth in nude mice

To examine the biological activity of the endogenously expressed MMP-9-PEX in the inhibition of tumor growth *in vivo*, the intracranial implantation was done using luciferase expressing cells parental (P-Luc), vector alone transfected cells (VC-Luc) or MMP-9-PEX transfected cells (PX1-Luc, PX2-Luc) in nude mice. Because the tumor cells express luciferase, tumor growth rates in the brain could be measured over time by measuring luciferase expression by bioluminescence. Tumor cells (1×10^6) were injected i.c. in to the brain of nude mice. To assess tumor growth, mice were imaged for bioluminescence after i.p. injection of D-luciferin. There was a significant decrease in bioluminescence in MMP-9-

PEX transfectants compared with control group (Fig 7a, e). After four weeks, mice were sacrificed, and tumors were removed, sectioned and histochemical analyses were performed. Each mouse injected with parental cells (P-Luc) and vector alone transfected cells (VC-Luc) developed tumors. In contrast, mice that were injected with MMP-9-PEX transfectants (PX1-Luc or PX2-Luc) showed tumor growth delay at four weeks post-injection and a decrease in tumor size when examined by H&E staining (Fig 7b). To determine whether the antitumor effects of MMP-9-PEX were caused by changes in angiogenesis, expression of CD31 and MMP-9 was analyzed in tumor sections of animals implanted with P-Luc, VC-Luc, PX1-Luc, and PX2-Luc glioma cells. MMP-9-PEX markedly reduced tumor vascularization as determined by CD31 staining (Fig 7c, d).

Discussion

The multiple biological functions of the MMP-9 are due to discrete structural features within the protein26 and we sought to determine the role of the MMP-9-PEX domain in glioma tumorigenesis. We preferred to express MMP-9-PEX in human glioblastoma cells using an expression vector to avoid the uncertainties in folding and modification associated with recombinant proteins produced in bacteria. In this report, we have shown that human MMP-9-PEX-engineered SNB19 cells can secrete biologically functional MMP-9-PEX protein capable of inhibiting MMP-9 activity and invasion. This concurs with previous studies that have shown the inhibition of activity of recombinant murine MMP-9 and a reduction in invasion of predominantly MMP-9 expressing human malignant melanoma A375 cells by recombinant murine MMP-9-PEX-GST fusion protein. Similarly, Brooks et al.,16 have shown that the avian MMP-2-PEX domain fusion protein blocks MMP-2 activity *in vivo*.

Angiogenesis was known to be essential for solid tumor growth and spread, and consequently became an attractive target against anti-tumor treatment. To investigate the potential role of MMP-9-PEX in angiogenesis, *in vitro* capillary-like structure formation studies were done using HMECs. Interestingly, MMP-9-PEX conditioned medium suppressed the ability of HMECs to form a capillary-like structure on Matrigel and this was further confirmed using purified MMP-9-PEX protein. Addition of exogenous recombinant MMP-9 partially reversed the inhibition caused by MMP-9-PEX suggesting that MMP-9-PEX mediates its functions in part through MMP-9 inhibition-independent pathways. We also have found that *in vitro* MMP-9-PEX strongly inhibited the migration of HMECs. These results demonstrate that MMP-9-PEX conditioned medium affects multiple steps in the angiogenic process. Similarly, previous studies have shown MMP-2-PEX fusion protein prevents the binding of MMP-2 to integrin αvβ3, thereby disrupting angiogenesis.16, 24 Among the molecules with specific effects on vascular endothelial cells, VEGF is considered to be the most powerful and specific growth factor responsible for tumor angiogenesis.34 We observed downregulation of MMP-9, VEGF and VEGFR2 transcripts as well as protein levels in HMECs by MMP-9-PEX conditioned medium. MMP-9-PEX could also achieve its antiangiogenic effects in part through blockade of the VEGF-VEGFR2 signaling pathway. Further studies will be conducted to elucidate the molecular basis of MMP-9-PEX-mediated suppression of VEGF and VEGFR2.

A number of fragments or cryptic domains of large proteins have been identified as angiogenesis inhibitors.35 Studies have shown that these proteins have the ability to inhibit endothelial cell function by increasing apoptosis.35–37 Thus, it seems reasonable to postulate that the induction of apoptosis may be a critical event in the antiangiogenic effect of MMP-9-PEX. Here, we investigated the potential role of MMP-9-PEX as a regulator of apoptosis. MMP-9-PEX conditioned medium increased subG_0- G_1 phase of the cell cycle and exhibited chromosomal condensation in HMECs. Caspases are critical components of

the apoptotic machinery and their activation play pivotal roles in both mitochondria and death receptor–mediated pathways.38 To elucidate the potential molecular mechanism, we assessed the *in vitro* expression of some apoptosis- associated molecules by immunoblotting. MMP-9-PEX conditioned medium treatment activates caspase-3, caspase-8 and caspase -9 and results in PARP cleavage. Caspase-3 is an executioner caspase that can be activated by other caspases including the intrinsic mitochondrial pathway involved caspase-9 and an extrinsic death-receptor pathway-associated caspase-8.39 The results reveal that MMP-9-PEX-induced apoptosis in HMECs is probably mediated in part, by both intrinsic and extrinsic caspase cascades.

In gliomas, the expression of MMP-9 correlates with tumor growth, invasion and angiogenesis.11¯13 We used a clinically relevant orthotopic implantation approach and found that secretion of MMP-9-PEX from stable transfectants in glioblastoma experimental tumors resulted in a reduction of the overall tumor mass. We further identified the anti-angiogenic effect as indicated by CD31 staining of tumor vascular endothelial cells. Similarly, other investigators also showed that MMP-2-PEX caused a marked decrease in tumor vessel density and inhibited tumor growth in subcutaneous melanoma and intracranial glioma tumor models.24, 40

In conclusion, the present study has shown that (*a*) enforced expression of MMP-9-PEX in human glioblastoma cells inhibited MMP-9 in both *in vitro* and *in vivo* experimental models (b) MMP-9-PEX can inhibit *in vitro* angiogenesis by decreasing the expression of VEGF and VEGFR2 in HMECs c) MMP-9-PEX conditioned medium induced apoptosis in HMECs as indicated by the activation of caspases and the induction of PARP cleavage and (*d*) MMP-9-PEX expression drastically reduced tumor growth in intracranial tumor model accompanied by a decrease in microvessel density. In summary, we provide compelling evidence that MMP-9-PEX protein expressed by engineered glioma cells possesses potent antiangiogenic properties that block glioma progression in an orthotopic experimental brain cancer model.

Acknowledgments

We thank Noorjehan Ali for technical assistance.

Grant sponsor: NIH Grant number NS-51625

References

1. Kleihues, P.; Cavenee, WK., editors. Pathology and genetics of tumours of the nervous system. Lyon: IARC Press; 2000.
2. Prados MD, Levin V. Biology and treatment of malignant glioma. Semin Oncol. 2000; 27:1–10. [PubMed: 10866344]
3. DeAngelis LM. Brain tumors. N Engl J Med. 2001; 344:14–23.
4. Bello, L.; Giussani, C.; Carrabba, G.; Pluderi, M.; Costa, F.; Bikfalvi, A. Angiogenesis and invasion in gliomas. In: Kirsch, M.; Black, PM., editors. Angiogenesis in brain tumors. Boston: Kluwer Academic Publishers; 2004. p. 263-284.
5. Holland EC. Glioblastoma multiforme: the terminator. Proc Natl Acad Sci USA. 2000; 97:6242–6244. [PubMed: 10841526]
6. Risau W. Mechanisms of angiogenesis. Nature. 1997; 386:671–674. [PubMed: 9109485]
7. Pepper MS. Extracellular proteolysis and angiogenesis. Thromb Haemost. 2001; 86:346–355. [PubMed: 11487024]
8. Parsons SL, Watson SA, Brown PD, Collins HM, Steele RJ. Matrix metalloproteinases. Br J Surg. 1997; 84:160–166. [PubMed: 9052425]

9. Nagase H, Woessner JF Jr. Matrix metalloproteinases. J Biol Chem. 1999; 274:21491–21494. [PubMed: 10419448]
10. Brew K, Dinakarpandian D, Nagase H. Tissue inhibitors of metalloproteinases: evolution, structure and function. Biochim Biophys Acta. 2000; 1477:267–283. [PubMed: 10708863]
11. Rao JS. Molecular mechanisms of glioma invasiveness: the role of proteases. Nat Rev Cancer. 2003; 3:489–501. [PubMed: 12835669]
12. Komatsu K, Nakanishi Y, Nemoto N, Hori T, Sawada T, Kobayashi M. Expression and quantitative analysis of matrix metalloproteinase-2 and -9 in human gliomas. Brain Tumor Pathol. 2004; 21:105–112. [PubMed: 15696970]
13. Hormigo A, Gu B, Karimi S, Riedel E, Panageas KS, Edgar MA, Tanwar MK, Rao JS, Fleisher M, DeAngelis LM, Holland EC. YKL-40 and matrix metalloproteinase-9 as potential serum biomarkers for patients with high-grade gliomas. Clin Cancer Res. 2006; 12:5698–5704. [PubMed: 17020973]
14. Overall CM. Matrix metalloproteinase substrate binding domains, modules and exosites. Overview and experimental strategies. Methods Mol Biol. 2001; 151:79–120. [PubMed: 11217327]
15. Allan JA, Docherty AJ, Barker PJ, Huskisson NS, Reynolds JJ, Murphy G. Binding of gelatinases A and B to type-I collagen and other matrix components. Biochem J. 1995; 309:299–306. [PubMed: 7619071]
16. Brooks PC, Silletti S, von Schalscha TL, Friedlander M, Cheresh DA. Disruption of angiogenesis by PEX, a noncatalytic metalloproteinase fragment with integrin binding activity. Cell. 1998; 92:391–400. [PubMed: 9476898]
17. Itoh Y, Takamura A, Ito N, Maru Y, Sato H, Suenaga N, Aoki T, Seiki M. Homophilic complex formation of MT1-MMP facilitates proMMP-2 activation on the cell surface and promotes tumor cell invasion. EMBO J. 2001; 20:4782–4793. [PubMed: 11532942]
18. Roeb E, Schleinkofer K, Kernebeck T, Pötsch S, Jansen B, Behrmann I, Matern S, Grötzinger J. The matrix metalloproteinase 9 (mmp-9) hemopexin domain is a novel gelatin binding domain and acts as an antagonist. J Biol Chem. 2002; 277:50326–50332. [PubMed: 12384502]
19. Bigg HF, Shi YE, Liu YE, Steffensen B, Overall CM. Specific, high affinity binding of tissue inhibitor of metalloproteinases-4 (TIMP-4) to the COOH-terminal hemopexin-like domain of human gelatinase A. TIMP-4 binds progelatinase A and the COOH-terminal domain in a similar manner to TIMP-2. J Biol Chem. 1997; 272:15496–15500. [PubMed: 9182583]
20. Wallon UM, Overall CM. The hemopexin-like domain (C domain) of human gelatinase A (matrix metalloproteinase-2) requires Ca2+ for fibronectin and heparin binding. Binding properties of recombinant gelatinase A C domain to extracellular matrix and basement membrane components. J Biol Chem. 1997; 272:7473–7481. [PubMed: 9054449]
21. Overall CM, King AE, Sam DK, Ong AD, Lau TT, Wallon UM, DeClerck YA, Atherstone J. Identification of the tissue inhibitor of metalloproteinases-2 (TIMP- 2) binding site on the hemopexin carboxyl domain of human gelatinase A by site-directed mutagenesis. The hierarchical role in binding TIMP-2 of the unique cationic clusters of hemopexin modules III and IV. J Biol Chem. 1999; 274:4421–4429. [PubMed: 9933646]
22. Patterson ML, Atkinson SJ, Knäuper V, Murphy G. Specific collagenolysis by gelatinase A, MMP-2, is determined by the hemopexin domain and not the fibronectin-like domain. FEBS Lett. 2001; 503:158–162. [PubMed: 11513874]
23. Tam EM, Moore TR, Butler GS, Overall CM. Characterization of the distinct collagen binding, helicase and cleavage mechanisms of matrix metalloproteinase 2 and 14 (gelatinase A and MT1-MMP): the differential roles of the MMP hemopexin C domains and the MMP-2 fibronectin type II modules in collagen triple helicase activities. J Biol Chem. 2004; 279:43336–43344. [PubMed: 15292230]
24. Bello L, Lucini V, Carrabba G, Giussani C, Machluf M, Pluderi M, Nikas D, Zhang J, Tomei G, Villani RM, Carroll RS, Bikfalvi A, et al. Black PM. Simultaneous inhibition of glioma angiogenesis, cell proliferation, and invasion by a naturally occurring fragment of human metalloproteinase-2. Cancer Res. 2001; 61:8730–8736. [PubMed: 11751392]
25. Giussani C, Carrabba G, Pluderi M, Lucini V, Pannacci M, Caronzolo D, Costa F, Minotti M, Tomei G, Villani R, Carroll RS, Bikfalvi A, et al. Bello L. Local intracerebral delivery of

endogenous inhibitors by osmotic minipumps effectively suppresses glioma growth *in vivo*. Cancer Res. 2003; 63:2499–2505. [PubMed: 12750272]

26. O'Connell JP, Willenbrock F, Docherty AJ, Eaton D, Murphy G. Analysis of the role of the COOH-terminal domain in the activation, proteolytic activity, and tissue inhibitor of metalloproteinase interactions of gelatinase B. J Biol Chem. 1994; 269:14967–14973. [PubMed: 8195131]
27. Cha H, Kopetzki E, Huber R, Lanzendorfer M, Brandstetter H. Structural basis of the adaptive molecular recognition by MMP9. J Mol Biol. 2002; 320:1065–1079. [PubMed: 12126625]
28. Van den Steen PE, Van Aelst I, Hvidberg V, Piccard H, Fiten P, Jacobsen C, Moestrup SK, Fry S, Royle L, Wormald MR, Wallis R, Rudd PM, Dwek RA, Opdenakker G, et al. The hemopexin and O-glycosylated domains tune gelatinase B/MMP-9 bioavailability via inhibition and binding to cargo receptors. J Biol. 2006; 281:18626–18637.
29. Jadhav U, Chigurupati S, Lakka SS, Mohanam S. Inhibition of matrix metalloproteinase-9 reduces in vitro invasion and angiogenesis in human microvascular endothelial cells. Int J Oncol. 2004; 25:1407–1414. [PubMed: 15492832]
30. Mohanam S, Chandrasekar N, Yanamandra N, Khawar S, Mirza F, Dinh DH, Olivero WC, Rao JS. Modulation of invasive properties of human glioblastoma cells stably expressing amino-terminal fragment of urokinase-type plasminogen activator. Oncogene. 2002; 21:7824–7830. [PubMed: 12420219]
31. Ezhilarasan R, Mohanam I, Govindarajan K, Mohanam S. Glioma cells suppress hypoxia-induced endothelial cell apoptosis and promote the angiogenic process. Int J Oncol. 2007; 30:701–707. [PubMed: 17273772]
32. Nuñez G, Benedict MA, Hu Y. Inohara N.Caspases: the proteases of the apoptotic pathway. Oncogene. 1998; 17:3237–3245. [PubMed: 9916986]
33. Thornberry NA, Lazebnik Y. Caspases: enemies within. Science. 1998; 281:1312–1316. [PubMed: 9721091]
34. Plate KH, Breier G, Weich HA, Risau W. Vascular endothelial growth factor is a potential tumour angiogenesis factor in human gliomas in vivo. Nature. 1992; 359:845–848. [PubMed: 1279432]
35. Tabruyn SP, Griffioen AW. Molecular pathways of angiogenesis inhibition. Biochem Biophys Res Commun. 2007; 355:1–5. [PubMed: 17276388]
36. Wahl ML, Kenan DJ, Gonzalez-Gronow M, Pizzo SV. Angiostatin's molecular mechanism: aspects of specificity and regulation elucidated. J Cell Biochem. 2005; 96:242–261. [PubMed: 16094651]
37. Tabruyn SP, Sorlet CM, Rentier-Delrue F, Bours V, Weiner RI, Martial JA, Struman I. The antiangiogenic factor 16K human prolactin induces caspase-dependent apoptosis by a mechanism that requires activation of nuclear factor-kappaB. Mol Endocrinol. 2003; 17:1815–1823. [PubMed: 12791771]
38. Logue SE, Martin SJ. Caspase activation cascades in apoptosis. Biochem Soc Trans. 2008; 36:1–9. [PubMed: 18208375]
39. Stupack DG, Cheresh DA. Apoptotic cues from the extracellular matrix: regulators of angiogenesis. Oncogene. 2003; 22:9022–9029. [PubMed: 14663480]
40. Pfeifer A, Kessler T, Silletti S, Cheresh DA, Verma IM. Suppression of angiogenesis by lentiviral delivery of PEX, a noncatalytic fragment of matrix metalloproteinase 2. Proc Natl Acad Sci USA. 2000; 97:12227–12232. [PubMed: 11035804]

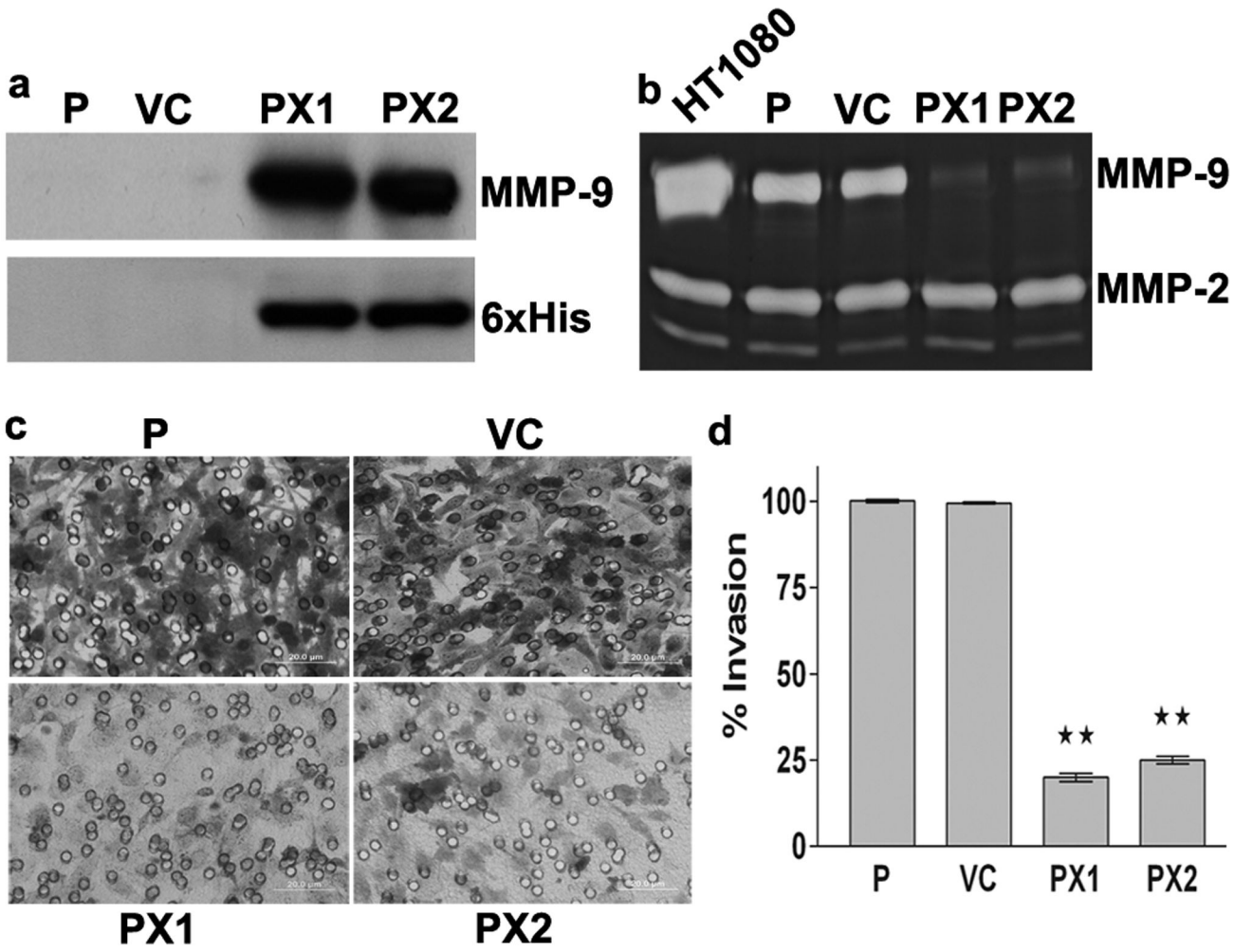

Figure 1.

Inhibition of MMP-9 activity and tumor cell invasion by MMP-9 PEX. (**a**) Western Blotting. SNB19 cells were transfected with either vector alone (VC) or MMP-9-PEX vector and stable transfectants (PX1, PX2) were selected. Conditioned media were analyzed by western blotting using anti-MMP-9 antibody or anti-His tag antibody. (**b**) Gelatin zymography. Parental and stable transfectants were cultured in growth medium supplemented with 200 nM phorbol myristate acetate (PMA) for 24-h. Conditioned medium obtained from PMA-treated parental (P), vector alone (VC) and MMP-9 PEX stable transfectants (PX1, PX2) and were resolved under nonreducing conditions on 10% SDS-PAGE gels. Gels were stained with amido black and areas of gelatinolysis were visualized as transparent bands. Conditioned medium from HT1080 cells was used to identify the gelatinolytic bands and their approximate molecular weights on the gels. (**c**) Matrigel invasion assay. Transfected SNB19 cells were assayed for invasive capacity in Matrigel coated tissue culture inserts for 24-h. Cells migrated to the bottom side of the insert were stained and photographed. Representative images are shown from one of three independent experiments with similar results. (**d**) Invasion index was determined as mean ± SD of three experiments done in duplicate. **p< 0.01 significantly different from vector alone transfected cells.

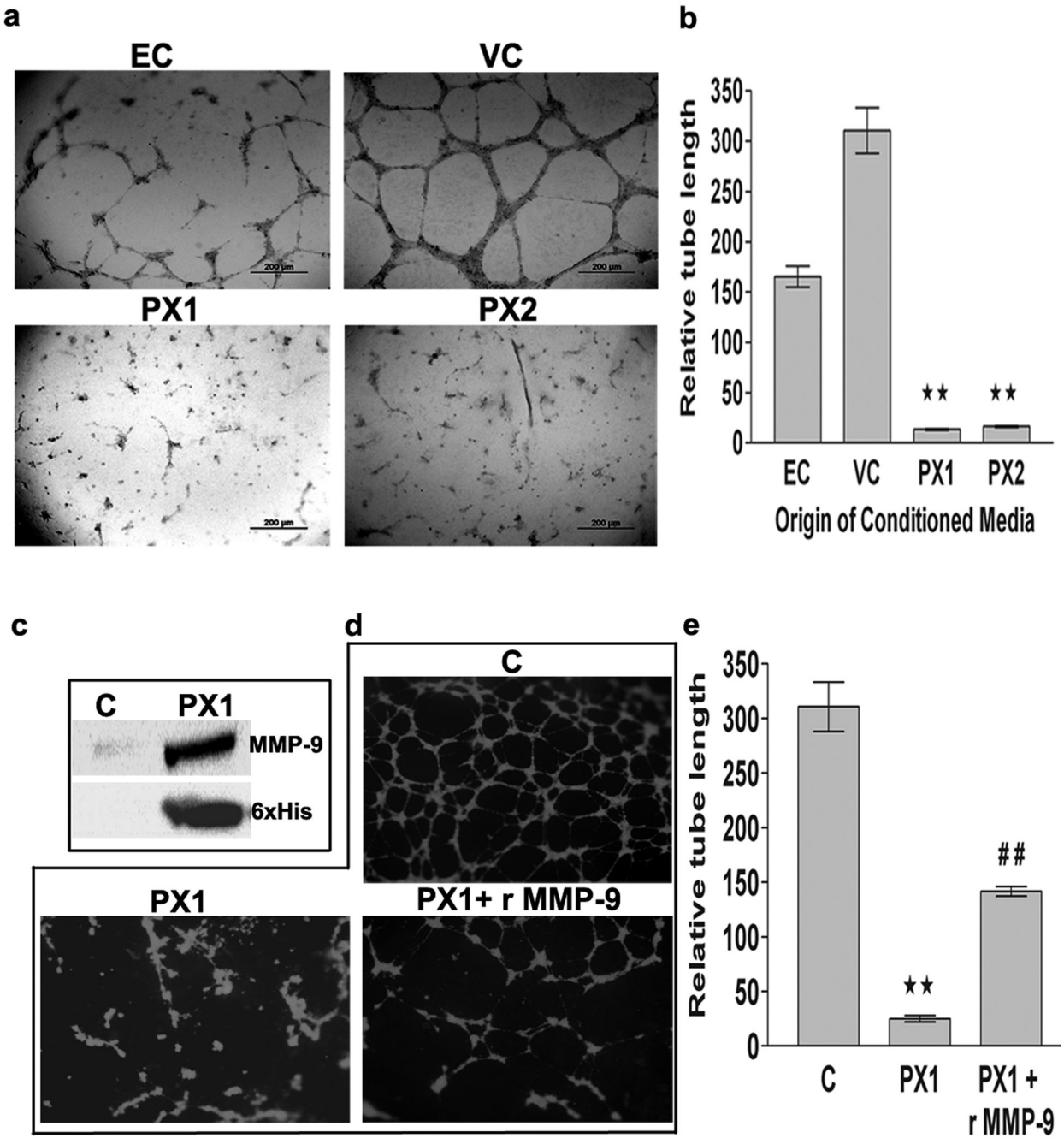

Figure 2.

In vitro angiogenesis assay. Matrigel was plated into flat-bottomed 96 well tissue culture plates and allowed to gel for 20 min at 37°C before HMECs were added. HMECs were grown in the presence of growth medium (EC) or conditioned medium collected from vector alone (VC) or MMP-9-PEX transfected SNB19 (PX1, PX2) cells for 24-h. (a) Cells were photographed using phase contrast microscopy; figures are representative of three independent experiments. (b) The capillary length was determined by computer-assisted image analysis with the Image-pro discovery program. The results are presented data as mean ±SD of three experiments done in triplicate. **p<0.01 (VC versus PX1 or PX2). (c) MMP-9-PEX was purified from serum-free medium collected from PX-1 cells using HisPur

cobalt resin and the homogeneity was confirmed using anti-MMP-9 or anti-His antibodies by western blotting. (d) *In vitro* angiogenesis assay was performed using the conditioned medium collected from parental SNB19 cells (C) or purified PX1 protein (1 μ g/ml) with and without recombinant MMP-9 (1 ηg/ml). (e) Graphical representation of data as mean ±SD of three experiments done in triplicate **$p< 0.01$ (C versus PX1) $^{\#\#}p< 0.01$ (PX1 versus PX1+ rMMP-9).

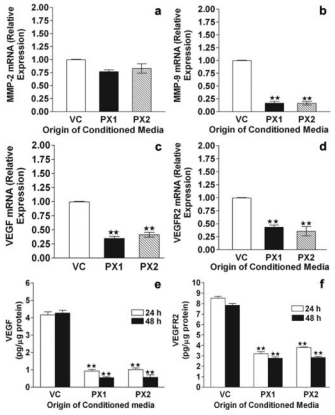

Figure 3.

Real time RT-PCR. HMEC cultures were exposed to vector alone (VC) or MMP-9-PEX SNB19 (PX1,PX2) cell conditioned medium for 24 h. Conditioned media were removed, cells were lysed, and total RNA extracted with Trizol Reagent. Reverse transcription reactions were carried out on total RNA with the cDNA cycle kit using the random primers. Gene transcripts for MMP-2 (**a**), MMP-9 (**b**), VEGF (**c**) and VEGFR2 (**d**) were measured using real-time reverse transcription-PCR. Transcript of β-actin was used as the internal control. Data represent a result of triplicate samples from two independent experiments. **p< 0.01. ELISA. HMEC cultures were exposed to vector or MMP-9-PEX SNB19 cell conditioned medium. Culture supernatants and lysates were subjected to the measurements for VEGF (**e**) and VEGFR2 (**f**) by ELISA respectively. Data represent a result of triplicate determinations from two independent experiments. **p< 0.01

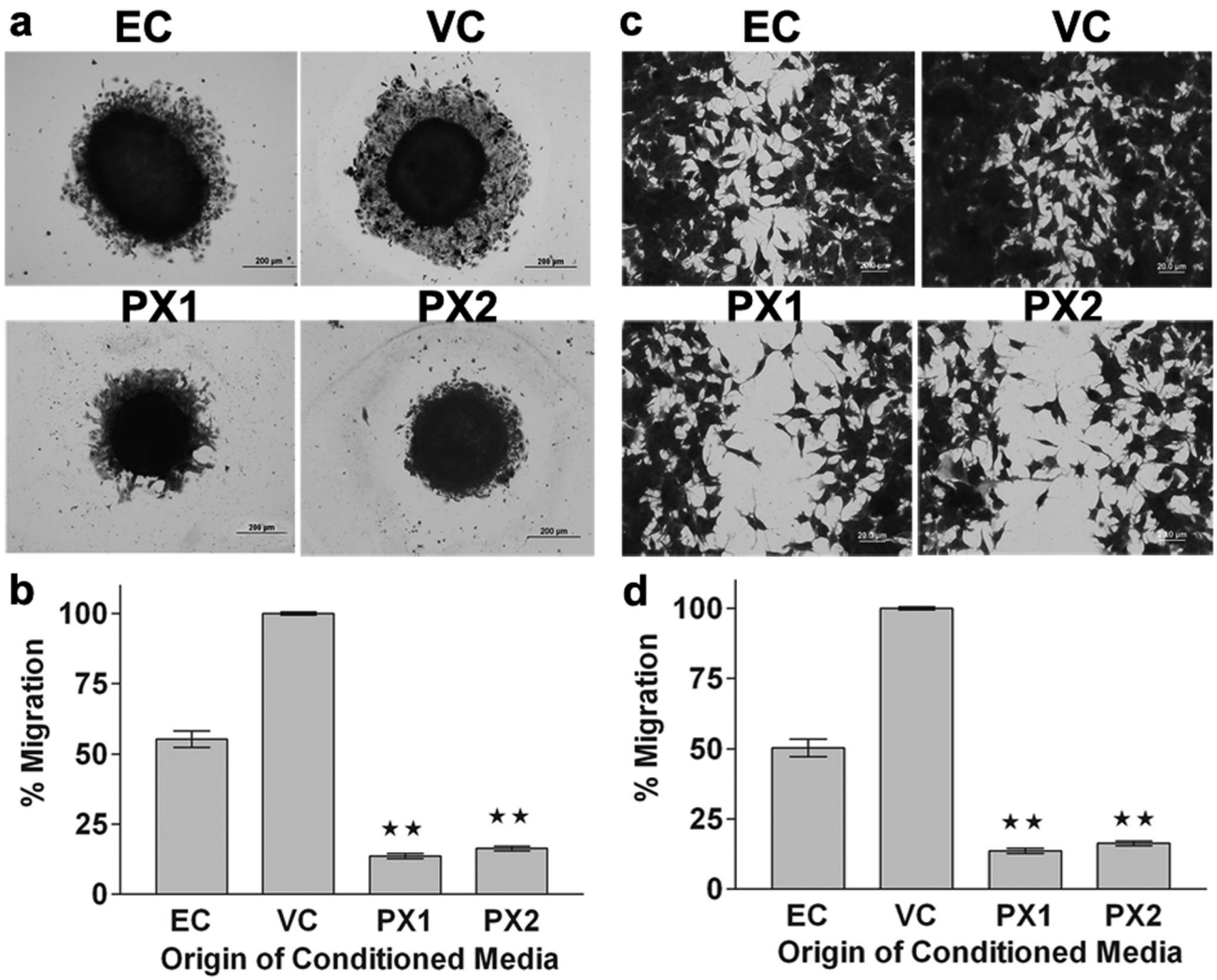

Figure 4.

MMP-9-PEX inhibits migration of HMECs. (**a**) Spheroid migration assay. Multicellular HMEC spheroids were cultured for 24-h in presence of vector alone (VC) or MMP-9-PEX transfected SNB19 (PX1, PX2) cell conditioned medium, after which the spheroids were fixed and stained with crystal violet. Cellular migration from the spheroids was assessed under light microscopy. Images are representative from three separate experiments. (**b**) Radial migration of cells from spheroids was quantitated and graphed. Data are as mean ±SD of three experiments done in triplicate. **p< 0.01. (**c**) Monolayer wound-induced migration assay. A line was scratched with a plastic pipette tip in HMEC cultures, washed twice with PBS, and the medium was replaced with vector alone (VC) or MMP-9-PEX SNB19 (PX1, PX2) cell conditioned medium. After 24-h exposure, cells that had migrated to the wounded areas were fixed, stained with crystal violet and counted under a microscope for quantification of cell migration. Images are representative from three separate experiments. (**d**) Migration was calculated as the average number of cells observed in five random high power wounded fields/per well. The results are presented as mean ±SD of three experiments done in duplicate. **p< 0.01

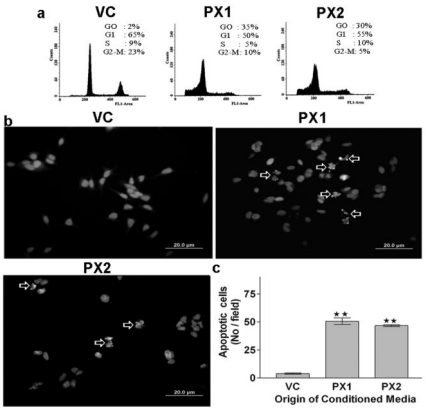

Figure 5.

Flow cytometry. (**a**) Effect of MMP-9-PEX on cell cycle distribution in HMECs. Cells were grown in vector alone (VC) or MMP-9-PEX SNB19 (PX1, PX2) cell conditioned medium for 24 hr and then the cells were harvested, stained with propidium iodide and cell cycle distribution was determined by flow cytometry. A representative cell cycle analysis is shown. Apoptosis evaluation. (**b**) Apoptosis was evaluated in HMECs at 24-h after exposure to vector alone (VC) or MMP-9-PEX SNB19 (PX1, PX2) cell conditioned medium by fluorescence microscopy using the chromatin stain Hoechst 33258. (**c**) The apoptotic index was quantitated by counting five random fields (in duplicate wells) per group. Data represent a result from two independent experiments. **p< 0.01

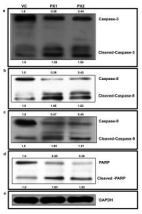

Figure 6.
Effects of PEX on apoptosis in HMECs. Endothelial cells were grown in vector alone (VC) or MMP-9-PEX SNB19 (PX1, PX2) cell conditioned medium for 24-h harvested and cell lysates were subjected to electrophoretic analysis through SDS-PAGE followed by transfer to nitrocellulose membrane. Western blot analysis was done with the indicated antibodies and representative samples were shown.

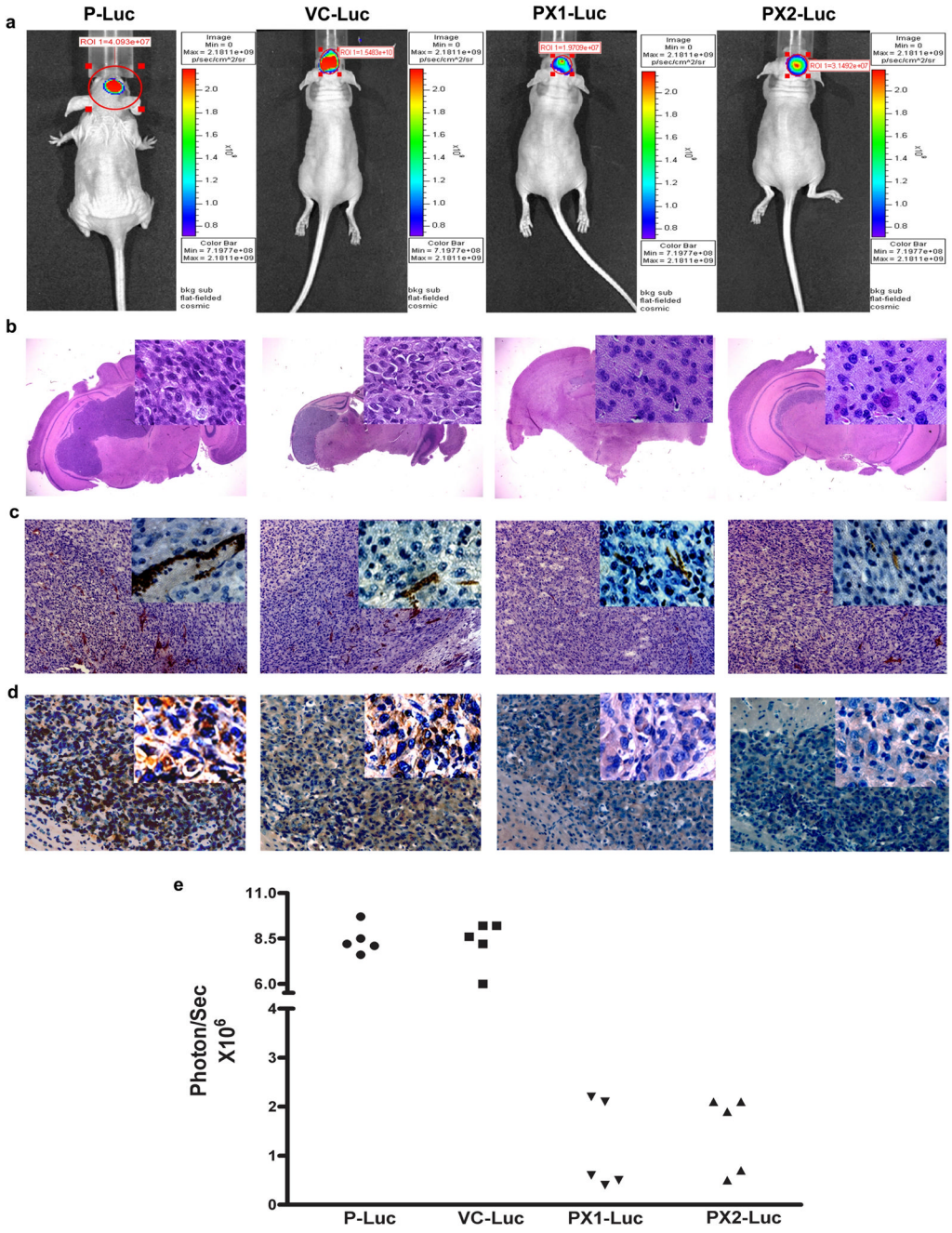

Figure 7.

Effect of MMP-9-PEX on the growth of intracranial SNB19 tumors (**a**) Bioluminescence imaging of SNB19 tumors *in vivo*. Parental (P), vector alone (VC) and MMP-9-PEX SNB19 transfectants (PX1, PX2) engineered to express luciferase by phCMV-Luc transfection were examined by optical imaging. A representative experiment shows the week four images of bioluminescence being obtained simultaneously from intracranial tumors of mice implanted of parental (P-Luc), vector alone (VC-Luc) or MMP-9-PEX SNB19 cells (PX1-Luc, PX2-Luc). (**b**) Photomicrograph of H&E staining from tumor sections. Insert, area that was magnified. (**c**) Immunohistochemistry of CD31 on xenografted tumors from parental SNB19 cells and stable transfectants (**d**) Analysis of xenografted tumors by immunohistochemical

staining using anti-MMP-9 antibody (**e**) Bioluminescence data corresponding to individual mice from animals intracranially implanted with parental (P-Luc, $n = 5$), vector alone (VC-Luc, $n = 5$) and MMP-9-PEX vector transfected (PX1-Luc, $n = 5$; PX2-Luc, $n = 5$) glioblastoma cells.